BENEFICIATION OF FLUXED TITANIFEROUS SLAG TO A MARKETABLE TITANIA PRODUCT BY THE MODIFIED UPGRADED SLAG PROCESS

[1]Xolisa Goso, [2]Jochen Petersen, [3]Merete Tangstad, [3]Jafar Safarian

Corresponding author email: XolisaG@mintek.co.za

[1]Mintek, Pyrometallurgy division, 200 Malibongwe Drive, Private Bag X3015, Randburg, 2125, South Africa

[2]University of Cape Town, Chemical Engineering Building, Private Bag X3, Rondebosch, 7701, South Africa

[4]Norwegian University of Science and Technology, Department of material science and engineering, N-7491 Trondheim, Norway

Keywords: Titaniferous magnetite, smelting, titaniferous slag, UGS process, synthetic rutile, titania pigment

Abstract

The current study involved investigations into the smelting production of a limestone fluxed titaniferous slag with a suitably low MgO chemistry for subsequent beneficiation using the modified Upgraded Slag (UGS) process to produce a marketable titania material. The smelting of titaniferous magnetite (titanomagnetite) mixed with a Sascarb reductant and synthetic limestone flux was conducted in a conventional graphite suscepting induction furnace inside an alumina crucible in argon atmosphere and a water-cold copper crucible induction furnace. The slag produced in alumina crucible was severely contaminated by alumina from the crucible wear – the abundant alumina promoted the crystallisation of the chemically inert magnesium alumina spinel. The slag produced in the cold copper crucible had high residual iron mostly from iron metal susceptor and non-equilibrium iron reduction reaction in the titanomagnetite – the vanadium primarily partitioned to the titaniferous slag. The high iron concentrations in the slag resulted in the crystallisation of an ulvospinel. The TiO_2 in the slag produced in alumina crucibles was upgraded using the unoptimised UGS process to a maximum of about 67%, which was significantly lower than the feedstock requirement for the production of the preferred chloride pigment – the main detrimental species were incorporated in the chemically inert spinel and excess alumina phases. The best UGS product with 90.45% TiO_2 was produced from the cold crucible induction furnace slag – the cumulative recovery of TiO_2 was 83%. Though the TiO_2 grade in this product was appreciably high, the SiO_2, Al_2O_3, CaO, and Cr_2O_3 concentrations were higher and the particle size distribution was finer than the feedstock specification for the chloride pigment production. Since the UGS product was mainly composed of rutile structure, it was not suitable for use as feed for the sulfate pigment production. It is shown that the optimisation of the UGS process conditions has a potential to reduce the impurities to levels suitable for use as feedstock for the preferred chloride pigment production process.

1. INTRODUCTION

1.1. Background

Titaniferous magnetite (titanomagnetite) deposits are defined as accumulations of ilmenite ($FeTiO_3$) and magnetite (Fe_3O_4) with a titania (TiO_2) concentration of more than 1wt%. Titanomagnetite is commonly concentrated with vanadium in the same mineral deposits (Fischer, 1975). In general, titanomagnetite contains economically appreciable vanadium and iron reserves, as well as significant titanium reserves. Thus, titanomagnetite offers a unique opportunity for use as a resource for three commodities, namely; vanadium, steel and titanium products. It is used as the primary source of vanadium throughout the world and a significant source of steel in countries like China and Russia (Roskill, 2010; Taylor, et al., 2006; Moskalyk & Alfantazi, 2003).

Titanomagnetite is typically processed by smelting in electric arc or blast furnaces (EAF or BF) in the presence of dolomite-quartz flux and carbonaceous reductant in order to produce a valuable vanadium bearing pig iron and a virtually valueless titanium bearing slag, referred to as titaniferous slag. The pig iron is processed further to produce vanadium and steel products. The titaniferous slag is a by-product that is generally discarded in waste dumps. Titaniferous slags have been produced as by products in many industrial operations around the world, including in New Zealand by New Zealand Steel (NZS) (produced from iron sands), in China by Panzhihua Iron and Steel Corporation (Pangang) and Chengde Iron and Steel (CHMP), in Russia by EVRAZ Nizhny Tagil Iron and Steel (NTMK), and in South Africa by the defunct EVRAZ Highveld Steel and Vanadium Corporation (EHSV) (Steinberg, et al., 2011; Zhang, et al., 2007; NTMK, 2003; Kelly, 1993). These slags are typically described by the TiO_2-SiO_2-Al_2O_3-MgO-CaO system, and contain between 8wt% and 40wt% TiO_2. Table 1 gives a summary of the typical chemical compositions of some titaniferous slags produced around the world.

Table 1: Chemical compositions of some titaniferous slags produced around the world (wt%)

Operation	FeO	MgO	Al_2O_3	SiO_2	CaO	**TiO_2**	**V_2O_5**
NZS*	2.11	13.3	17.8	15.2	15.9	**32.1**	**0.20**
Pangang#	nr	7.0	14.0	22.0	27.0	**22.0**	**nr**
NMTK and CHMP*	0.6-1.0	11-13	14-15	28-30	30-32	**8-10**	**0.18-0.30**
EHSV+	1.0	14.1	18.0	16.2	14.1	**35.6**	**0.90**

*(Hassell, et al., 2016) , # (Sui, et al., 2004), +(Steinberg, et al., 2011), nr – not reported

The sizes of the titaniferous slag dumps have accumulated to massive stockpiles over the years of operations. For example, the titaniferous slag dump at Pangang was estimated to be above 50 million tonnes already in 2004, and was increasing at a rate of about 3 million tons per annum (Sui, et al., 2004); and the size of the titaniferous slag dump left behind by the defunct EHSV is estimated to be about 45 million tons (Africa, Mining review, 2017).

Amongst other valuables in titaniferous slags, the TiO_2 grades are attractive for upgrading to marketable titania products. Successful valorization of these slags would alleviate the environmental impact presented by the huge industrial waste stockpiles, improve the overall metallurgical process economics and maximise the exploitation of valuable resources. Titania (TiO_2) is the primary material of titanium, and is mainly used as pigment for various industrial applications including in paint, plastic and paper industries. The titania pigment is produced via one of two processes, namely; the sulfate and chloride processes. The chloride process is

preferred because it is relatively cheaper – in 2014, about 60% of the 4.5 million tons of titania pigment produced in the world was generated by the chloride process. However, the feedstock requirements for the chloride process are more stringent, for example; coarser particle size distribution of -850+106 µm, and chemical grade of >85% TiO_2, <0.13% CaO, <0.6% V_2O_5, and <2% SiO_2 (Gazquez, et al., 2014; Roskill, 2003; Van Dyk, 1999).

1.2. Introduction

The chemical components of the titaniferous slags generally occur in complex mineral phases such as titanaugite (TiO_2-SiO_2-Al_2O_3-MgO-CaO-V_2O_5), perovskite ($CaTiO_3$), pseudobrookite [$(Mg,Al,Ti,V)_3O_5$] diopside [$(Ca,Mg,Ti)_2(Si,Al,Ti)_2O_6$], and spinel [$Mg(Al,Ti,V)_2O_4$]. Though the titania grades in titaniferous slags are attractive for upgrading to marketable titania products like feedstock for the production of chloride pigment, these slags are still not processed further because they contain low TiO_2 and higher impurity grades than the feedstock requirements for production of the pigment, and have complex phase chemistry that cannot be handled by the available titania slag upgrading technologies (Pistorius, 2011; Van Vuuren & Tshilombo, 2011). Nevertheless, several complex processes have been proposed for processing low titania resources, including titaniferous slags, to marketable titania materials for use as direct pigment or as feedstock for the production of the preferred chloride pigment (Hassell, et al., 2016; Van Vuuren & Tshilombo, 2011; Xiao-hua, et al., 2008; Zhang, et al., 2007; Fouad, 2005; Becker & Dutton, 2002; Goso, et al., 2016a). Becker and Dutton (2002) patented a modified sulfate process for the valorization of the EHSV titaniferous slag. The process involved the contacting of slag with sulfuric acid in order to produce titanyl sulfate, followed by hydrolysis to produce titanyl hydroxide and calcination to produce titania pigment (Becker & Dutton, 2002). Xiao-hua et al. (2008) investigated the leaching kinetics of TiO_2 from the Pangang titaniferous slag using sulfuric acid as lixiviant in a similar sulfate process. Hassell et al. (2016) patented a similar version of the sulfate process for beneficiation of titanium-bearing materials.

Van Vuuren and Tshilombo (2011) proposed an alternative process for the beneficiation of titaniferous materials with EHSV titaniferous slag. In this process, the slag is subjected to selective nitriding at high temperatures and excessive reducing conditions, followed by relatively low temperature chlorination of titanium nitride to produce liquid titanium tetrachloride, which is beneficiated further using conventional processes to produce the titania pigment (Van Vuuren & Tshilombo, 2011). Fouad (2005) proposed another alternative process involving the application of the conventional sulfation roasting and leaching process for the removal of impurities from low grade titania resources using low grade ilmenite slag. In another process option, Zhang et al. (2007) aerated the molten titaniferous slag in order to grow the perovskite phase in the Pangang slag. The perovskite is recoverable from the slag by flotation (Zhang, et al., 2006; Wang, et al., 2006). Wang et al. (2006) showed that the TiO_2 can be recovered from the perovskite concentrate by the alkaline roasting method followed by leaching removal of Ca and other impurities.

As another option, Goso et al. (2016a) proposed the use of the established Upgraded Slag (UGS) process for the beneficiation of the titaniferous materials, which typically contain high concentrations of alkaline earth impurities. The UGS process is used commercially at Rio Tinto Fer et Titane (RTFT) in Canada for upgrading the SORELSLAG® generated from the Allard Lake ilmenite that contains relatively high levels of alkaline earth impurities (Borowiec, et al., 1998; Doan, 1996). In their investigations, Goso et al. (2016a) showed that the modified UGS process can increase the TiO_2 concentrations of 33% and 58% in respective fluxed and fluxless titaniferous slags to 75% TiO_2. In both UGS products, the major impurities were

magnesium and aluminium that were contained in a chemically inert magnesia alumina spinel ($MgAl_2O_4$) (Goso, et al., 2016a).

These processes for beneficiating titaniferous materials, including titaniferous slags, have not been implemented because they are not economically viable and some of these processes produce materials of still insufficient TiO_2 grades to qualify as useful titania products. Amongst these processes, the modified UGS process was one of the promising options. The UGS technology is relatively simple and is already in commercial operation. The operational principles of the UGS process are described in the open literature (Borowiec, et al., 1998). However, to stand a chance of producing a marketable titania product from titaniferous slag using the modified UGS process, the fluxing strategy during the primary smelting process needs to be reviewed in order to avoid the solidification of the chemically inert spinel.

The current study aimed to modify the fluxing strategy during smelting in order to produce a titaniferous slag with little or no spinel, followed by beneficiation using the modified UGS process. Jochens (1967) and Goso et al. (2016b) showed that the smelting of a South African titanomagnetite to produce a by-product slag containing a high CaO/ MgO ratio would crystallize perovskite as the primary phase, followed by rutile and diopside. Moreover, Goso et al. (2016b) showed that the phase assemblage of the reviewed slag compositions with more than 5% MgO would include the spinel at solidus state – the amount of the spinel in the slag would depend on the amount of MgO present. Thus, the approach of the current study involved the smelting of titanomagnetite in a magnesium deficient system in order to avoid or minimize the crystallization of the chemically inert spinel. In general, the magnesium dissolved in the slag originates mainly from the dolomite flux, and to a lesser extent from the titanomagnetite feed and the furnace refractory. Hence, the current study investigated the use of limestone as an alternative flux. The limestone fluxed titaniferous slag was thus subjected to the best conditions of the modified UGS process developed in previous work (Goso, et al., 2016a).

2. EXPERIMENTAL PROCEDURES

2.1. Materials

A titanomagnetite ore mined from the main magnetite layer (MML) of the South Africa's Bushveld complex was supplied in the past by the defunct EHSV. The titanomagnetite ore was subjected to elementary concentration by low intensity magnetic separation (LIMS) in order to minimise the MgO in the feed to smelting during the production of a titaniferous slag with minimum MgO content. A low sulfur carbonaceous material or Sasol carbon, with the trade name 'LS SASCARB', (Sascarb) was supplied by Sasol and used as a reductant in the testwork. Chemical grade MgO, Al_2O_3, SiO_2 and CaO were supplied by Associated Chemical Enterprise and used as synthetic fluxes during the smelting of the MML titanomagnetite concentrate. The bulk chemical compositions of the materials used in the study are included in Table 2.

Analytical reagent (AR) grade HCl concentrate (37%) and NaOH pellets (99%) were used to prepare the respective lixiviants. De-ionised water was used for making up the lixiviants and washing the residues.

Table 2: Bulk compositions of the titanomagnetite materials, reductant, fluxes and other reagents (wt%)

	Titanomagnetite ore	Titanomagnetite concentrate	Sascarb	MgO	Al_2O_3	SiO_2	CaO
*Fe_3O_4	77.7	77.9					

MgO	1.48	1.34		99			
Al_2O_3	3.97	4.17			98		
SiO_2	1.34	1.25				98.5	
CaO	0.07	<0.05					96
$^{\$}TiO_2$	13.3	13.2					
V_2O_5	1.67	1.86					
Cr_2O_3	0.20	<0.05					
MnO	0.24	0.30					
C			98.7				
Ash			0.33				
LOI**			0.97				

*Total Fe expressed as Fe_3O_4; <0.05wt%: analyte concentration is below the detection limit, which is 0.05wt%; $^{\$}$Titanium species ($Ti^{3+}$ and Ti^{4+}) expressed as TiO_2

** Loss of ignition

2.2. Equipment

The smelting of titanomagnetite concentrate to produce a spinel free titaniferous slag for beneficiation studies was first conducted in a 25 kW induction furnace. This furnace was setup at Mintek by LH power. A schematic diagram showing the induction furnace set up is demonstrated in Figure 1.

In order to avoid the contamination of the titaniferous slag by the alumina crucible during smelting, a water-cooled cold copper crucible in a high frequency induction furnace located at the Norwegian University of Science and Technology (NTNU) in Norway was used. This furnace facility is a creation of a combination of several components from different suppliers: a power supply from Farfield Electronics (Pty) Ltd and a water-cooled copper crucible from Australian Nuclear Science and Technology Organization (ANSTO). The power capacity of this induction furnace is rated at 75 kVA. A schematic representation of the crucible setup is shown in Figure 2.

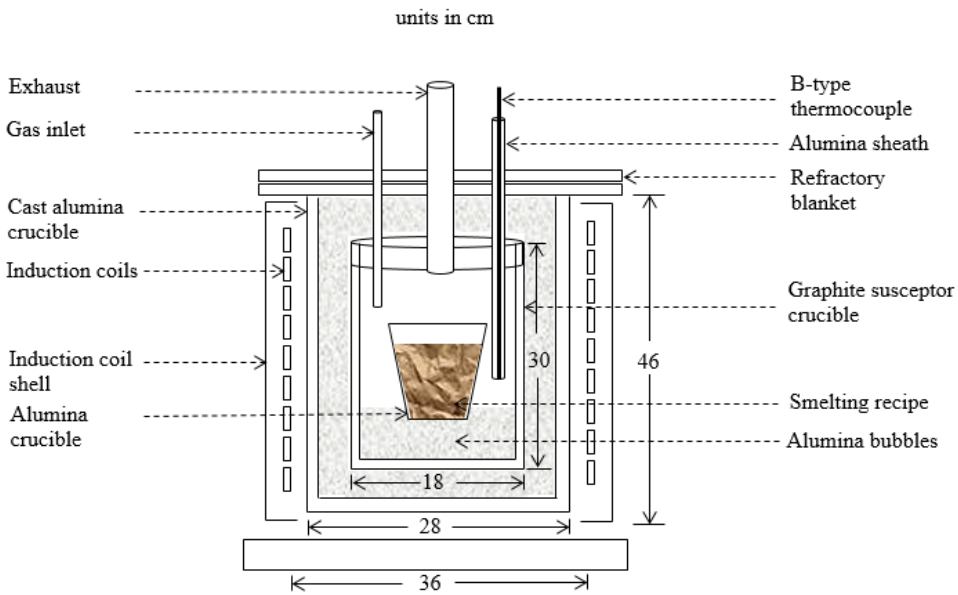

Figure 1: Schematic diagram of the 25 kW induction furnace setup

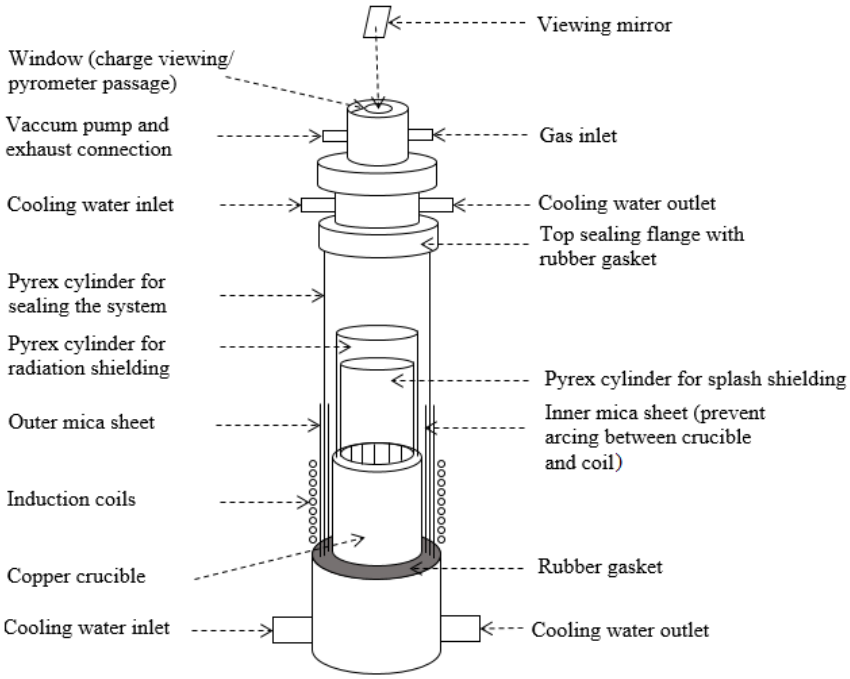

Figure 2: Schematic representation of the crucible setup in the cold crucible induction furnace

The bulk chemical analysis of samples in the testwork were conducted by a Varian Vista-PRO CCD simultaneous Inductively Coupled Plasma Optical Emission Spectrometer (ICP-OES) and CS744 LECO instrument. The mineralogical characterization of the samples was conducted by a Bruker D8 advanced X-Ray Diffractometer (XRD) and Zeiss EVO® MA15 scanning electron microscope (SEM) coupled with a Bruker energy dispersive spectrometer (EDS) operated with Bruker Esprit software.

2.3. Production of titaniferous slag

The titanomagnetite concentrate was smelted in alumina crucibles in the presence of Sascarb reductant and synthetic flux to target a titaniferous slag with minimum or no spinel formation. The reductant addition was calculated using Equations [1] and [2]. Based on previous testwork conducted in the same laboratory (Maphutha, et al., 2017), the stoichiometric reductant addition in the smelting recipe was maintained at 110%.

$$Fe_3O_4 + 4C = 3Fe + 4CO \quad [1]$$

$$V_2O_5 + 5C = 2V + 5CO \quad [2]$$

The fluxing strategy adopted in the current smelting testwork aimed to achieve a titaniferous slag with minimum or no crystallisation of the spinel. Moreover, in order to relate to the phase diagram for synthetic titaniferous slags (Jochens, 1967; Goso, et al., 2016b), the amounts of SiO_2 and Al_2O_3 in the smelting recipe and the overall flux size (for TiO_2 control) were adjusted such that the subsequent titaniferous slag would have an approximate chemical composition of: SiO_2 = 20wt%, Al_2O_3 = 13wt% and TiO_2 = 37wt%. CaO was added to act as the synthetic calcined limestone flux. When the smelting was conducted in the presence of an MgO-free flux while the flux size was maintained, it was anticipated that a titaniferous slag with MgO: CaO mass ratio of 4:26 would be produced. The MgO would only come from the titanomagnetite concentrate.

At first, the smelting test was conducted in the conventional induction furnace at a scale of 1000 g of titanomagnetite concentrate in order to produce sufficient sample for the subsequent slag beneficiation testwork. Individual recipes were charged into graphite and alumina crucibles - smelting in the graphite crucible was conducted to avoid contamination of the titaniferous slag by the alumina crucible. Each charged crucible was placed onto the conventional induction furnace as shown in Figure 1. The power of the induction furnace was gradually increased such that the sample was smelted at 1600°C for an hour before cooling down to room temperature. The heating cycle of the samples was conducted in an Ar atmosphere. The smelting products were cooled down by switching off the induction furnace power supply while the cooling water circuit and the Ar flow were left open during cooling. On completion of the testwork, alloy and slag samples were prepared and analysed by ICP-OES and LECO. The slag samples were also subjected to mineralogical characterisation by XRD and SEM-EDS.

The smelting tests in the cold crucible were conducted in triplicate at 300 g scale because of a limitation in the crucible size. The respective smelting recipes were mixed by milling in a ring mill to produce a homogeneous feed for smelting. In each test, the smelting recipe was quantitatively transferred into the copper crucible that was coated with boron nitride to avoid the leaking of the finely ground feed or molten charge and to facilitate the removal of the charge from the crucible after the test. A mass of 20 g of the Fe metal was placed on top of the smelting inside the cold crucible furnace to act as a susceptor. The smelting of the feed was conducted under Ar gas by increasing the power of the furnace to 80% capacity and allowed the test to continue for 10 minutes. The reactions inside the crucible were vigorous in the first 5 minutes and subsequently slowed down until there was no activity after 8 minutes – the test was left for an additional 2 minutes to ascertain that no further reaction took place. During smelting, the Fe metal susceptor would melt and descend to the bottom of the crucible while heating and melting the charge underneath. The recipe melted and produced a titaniferous slag and pig iron, which was diluted by the settling of the Fe metal susceptor. There was no available option for the measurement of the melt temperature during the tests. However, visual inspection of the melt inside the cold crucible was deemed satisfactory for the purpose of the production of the titaniferous slag for subsequent beneficiation testwork. The furnace power was shut off and the water circuits were left open in order to allow for the products to cool down. The products were collected and subjected to characterisation as described in the case of the smelting products of the conventional induction furnace above. The three batches of titaniferous slags were blended in order to have a sufficient sample for the subsequent UGS testwork

Table 3 gives a summary of the smelting recipes and conditions in both induction furnaces.

Table 3: Summary of the normalised smelting recipes (wt%) and some test conditions

Test	Titanomagnetite concentrate	Sascarb	CaO	Al_2O_3	SiO_2	Fe metal Susceptor	Induction Furnace	Crucible
1	73.58	13.80	7.68	0.44	4.49		Conventional	graphite
2	73.62	13.80	7.65	0.44	4.49		Conventional	alumina
3	68.53	12.81	7.12	0.42	4.17	6.94	Cold crucible	Copper
4	68.51	12.77	7.11	0.42	4.19	7.01	Cold crucible	Copper
5	68.57	12.81	7.14	0.42	4.18	6.88	Cold crucible	Copper

Generic material balance methodologies used by Maphutha et al. (2017) were adopted in the current study in order to determine the partitioning of the respective chemical elements between product streams. A block diagram showing the smelting process followed in the current study

is shown in Figure 3. The induction furnace smelting process can be described by the mass balance equation used for a batch process as shown in Equation [3]. This equation was deemed appropriate as there was no accumulation in the process – the mass of the titaniferous slag is determined by difference. The recoveries of the chemical elements of the feed material to the product streams were calculated using Equation [4]. In this context, recovery refers to the quantity or percentage of the particular chemical element contained in the feed that reports to one of the product streams, i.e. off-gas, slag or alloy, after the smelting process.

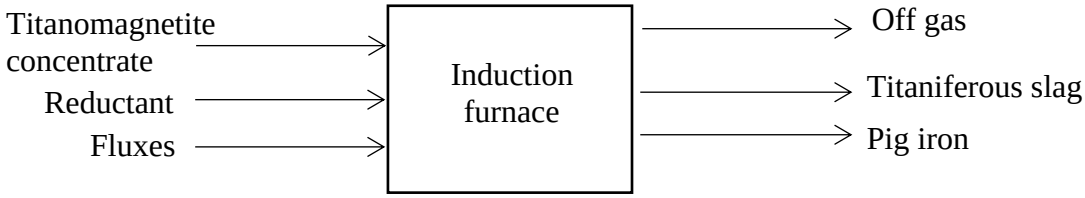

Figure 3: Block diagram of the smelting test in an induction furnace

$$\sum Mass\ in = \sum Mass\ out \qquad [3]$$

Where, '$\sum Mass\ in$' denotes the sum of the feed masses to furnace (titanomagnetite concentrate, reductant and fluxes), and '$\sum Mass\ out$' denotes the sum of the product masses from furnace (off-gas, titaniferous slag and pig iron).

$$\%Recovery\ of\ element\ i\ in\ a\ product\ stream = \frac{M_i\ in\ a\ product\ stream}{M_i\ in\ the\ feed} \times 100 \qquad [4]$$

where, 'M_i' is the mass of element i.

2.4. Beneficiation of titaniferous slags by the modified UGS process

The conventional UGS process involves: sampling and sizing of the titania bearing slag, oxidation of the sized slag, strictly controlled reduction of the oxidised slag, high temperature and pressurised HCl leaching of the roasted slag to remove impurities, and calcination of the solid residue to produce a high purity TiO_2 product suitable for use as feedstock for chloride pigment production (Borowiec, et al., 1998; Doan, 1996). In cases where the titania bearing slags contain high silica concentrations, a penultimate caustic soda leaching stage is added for silica removal (Doan, 1996).

In the current study the best scoping UGS conditions determined by Goso at al. (2016a) on processing the EHSV titaniferous slag were adopted. These unoptimised UGS process conditions included sizing the titaniferous slag to 150-600 µm particle size distribution (PSD); fluidised bed roasting of the sized slag of 100 g in mass in an oxidising atmosphere of air at 875°C for 2 hours; reduction in an atmosphere of CO at 875°C for 0.5 hours; leaching with 20wt% HCl lixiviant under refluxing at 110°C for 24 hours in a pulp density with s: l ratio of 1:4; caustic leaching with 2.15 M NaOH lixiviant at 100°C for 3 hours at a pulp density with s: l ratio of 1:4, and; calcination at 900°C for 3 hours. Bulk chemical and mineralogical analyses using ICP-OES, XRD and SEM-EDS as well as PSD examination were conducted at different stages during the UGS processing of the titaniferous slags.

In case of UGS processing of the titaniferous slag composite produced from the cold crucible induction furnace, the effects of HCl and NaOH leaching times on the titania grade of the

residue were evaluated by conducting leaching tests for 4, 24, and 48 hours in case of HCl leaching, and 1, 3, and 24 hours in case of NaOH leaching.

The recoveries of TiO_2 to the residue stream after HCl and NaOH leaching stages were based only on the residue analysis – the recoveries to the leachate were determined by difference. The TiO_2 recovery to the residue was calculated using Equation [5].

$$\%\,\mathrm{TiO_2}\ recovery\ to\ residue = \frac{\%\mathrm{TiO_2}_{residue} \times Mass_{residue}}{\%\mathrm{TiO_2}_{feed} \times Mass_{feed}} \times 100 \qquad [5]$$

3. RESULTS AND DISCUSSION

3.1. Physical appearance and masses of the smelting products

When the smelting was conducted using a graphite crucible, the separation of the alloy and slag was unsatisfactory. The poor separation was attributed to the reduction of Ti^{4+} and Ti^{3+} species by graphite to Ti(O,C) species which have high liquidus temperatures (Steinberg, 2008). Test 1 products were therefore not beneficiated for titania production in downstream processing.

The typical appearances of the smelting products produced using alumina and cold crucibles are shown in Figure 4 and Figure 5, respectively. The smelting of titanomagnetite in an alumina crucible resulted in a good separation between the slag and pig iron. During smelting in the cold crucible, not all the charge inside the crucible reacted to form the pig iron and the target titaniferous slag – some of the feed recipe formed a freeze lining inside the crucible as a consequence of the continuous cooling on the surface of the copper crucible. Hence, the smelting test in this furnace essentially produced four products, namely; (1) the off gas that is primarily composed of CO produced as a consequence of the reduction reactions, (2) the freeze lining, (3) the pig iron that is made up of the Fe metal added for induction purposes and, Fe and V produced according to Equations [1] and [2], and (4) the titaniferous slag. The slag contained some alloy entrainments. For the direct measurements of the masses of the freeze lining, alloy and slag, efforts were made to separate these materials the best way that is practically possible.

Figure 4: Photograph showing the appearance of the bulk smelting products in alumina crucible

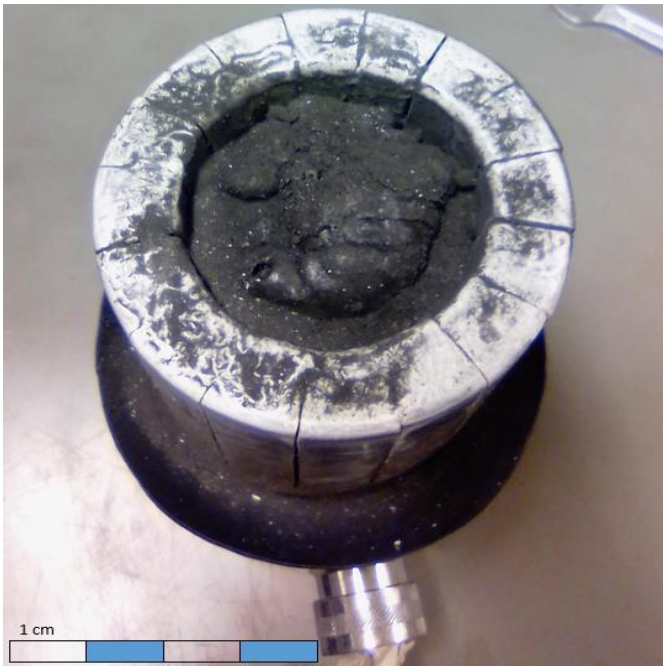

Figure 5: Typical appearance of the smelting test products in the cold copper crucible

The masses of the smelting test products are summarised in Table 4. The mass loss is primarily attributed to the emission of CO as per the chemical reactions shown in Equations [1] and [2]. In case of Test 2 conducted in the alumin crucible, the actual distributions of the masses in the products are fairly similar to theoretical masses.

In case of the triplicate tests conducted in the cold crucible induction furnace, the alloy masses suggest that there was about 80% metallisation of Fe from the titanomagnetite – this view assumes that the starting 20 g of the Fe susceptor was quantitatively recovered. Based on this estimation, the reported freeze lining contents of about 13% are lower than the anticipated contents of about 20%. Some of the unreacted recipe was ejected out of the copper crucible, as it appears on the brim of crucible shown in Figure 5 – the ejection of the unreacted sample was attributed to the violent nature of the smelting reaction in the cold crucible induction furnace. The mass losses presumably due to CO emissions were determined by difference; hence, the mass losses were consequently overestimated.

Table 4: Measured masses for the experiments (wt%).

Test	Mass loss	Freeze lining	Alloy	Slag
1*	32.53	-	0.00	67.47
2	30.67	-	45.56	23.77
3	28.48	13.13	36.04	22.34
4	30.27	12.62	35.60	21.51
5	28.53	13.03	36.05	22.39

*Failed test due to the lack of separation between slag and alloy, -not present

3.2. Chemical compositions of the smelting products

The bulk chemical compositions of the pig iron produced in the smelting tests are included in Table 5. For comparison, the chemical composition of a typical pig iron produced by the defunct EHSV is also included in Table 5. At EHSV, the successful furnace control system

involved the production of pig iron with the concentrations of C, V and Ti of 3.5wt%, 1.5wt%, 0.18wt%, respectively. When the desired chemical composition of the alloy was achieved, the process was said to be 'chemistry satisfactory' (Steinberg, 2008).

In the test completed in the alumina crucible, i.e. Test 2, the pig iron had significantly high concentrations of C and Ti, indicating that the smelting conditions were highly reducing. In the industrial operation at EHSV, excessive reducing conditions proved to be energy intensive and also resulted in the reduction and dissolution of unintended components of the melt into the pig iron. At this operation, mill-scale was used as a correction material to dilute the intensity of the reducing conditions and control the furnace energy input (Steinberg, 2008). Under the excessive reducing conditions suggested for Test 2, the pig iron also contained high concentrations of the slag forming species such Mg, Al, Si, Ca and Ti – this observation suggested a possible mixing of the slag and pig iron in the analysed samples. The low totals of chemical analysis results of pig iron produced in Test 2 were attributed to measurement uncertainty and the possible presence of oxide/slag inclusions.

The chemical analysis results of the pig iron produced in the cold crucible furnace, i.e. Test 3 to Test 5, reported lower C and V concentrations than the 'chemistry satisfactory' composition achieved by EHSV. These results suggest that the smelting conditions were not adequately reducing and/ or the reduction reactions were far from reaching equilibrium. The presence of a substantial freeze lining material and low Fe metallisation degrees of 80% support the view that the conditions were definitely not at equilibrium. The smelting in the cold crucible induction furnace stopped as soon as the induction metal settled at the bottom of the crucible. The suspended slag and freeze lining material were not effective for suscepting the energy from the induction coils. Hence, the smelting testwork was inevitably stopped far from the equilibrium state.

Table 5: Chemical compositions of the pig iron produced in the replicate tests (wt%)

Test	Mg	Al	Si	Ca	Ti	V	Cr	Mn	Fe	C	Total
EHSV	-	-	0.20	-	0.20	1.29	0.34	-	94.50	3.20	99.70
2	0.07	0.41	1.37	0.54	1.70	0.94	0.45	0.34	87.69	4.17	97.80
3	0.01	0.03	<0.025	0.01	0.04	0.08	0.10	0.10	98.03	1.54	99.94
4	0.02	0.03	<0.025	0.02	0.04	0.08	0.11	0.11	98.13	1.54	100.08
5	0.02	0.04	<0.025	0.09	0.14	0.02	0.03	0.02	97.95	1.46	99.77

<0.025%: analyte concentration is below the detection limit, which is 0.025wt% in the analytical method

The bulk chemical compositions of the titaniferous slags produced in the current study and the target slag are given in Table 6. The Al_2O_3 concentration in the titaniferous slag produced in the conventional induction furnace is significantly higher than the target. This is an indication of a severe contamination by Al_2O_3 from the crucible erosion as anticipated from previous studies (Maphutha, et al., 2017). Thus, the concentrations of the other components of the slag were diluted by Al_2O_3. In Table 6, the would-be chemical composition of the slag without Al_2O_3 contamination was calculated and included as Test 2*. The calculated chemical species are still significantly different from the targeted composition – particularly for SiO_2, CaO and TiO_2. This deviation was attributed to the uncharacteristically high iron content in this slag under the excessive reducing conditions (confirmed by high Ti and C in the pig iron).

The FeO content in the three titaniferous slags produced in the cold crucible induction furnace are consistently higher than the target composition. The high FeO concentrations in the slags support the assumption that the respective smelting tests did not reach the equilibrium state.

The concentrations of other components of the slags were significantly diluted by the high iron concentration. Moreover, it appears that the chemical compositions of the produced titaniferous slags, particularly the FeO and V_2O_5 content, are not comparable to typical titaniferous slags. The properties of the slag may also be distorted from that of the typical titaniferous slag. However, in the absence of a better option, the respective slags were processed further for the purpose of testing the efficiency of the UGS process for the beneficiation of titaniferous slags. The respective product slags were combined to make one composite sample for the downstream processing. In these tests, the recoveries of vanadium and titanium to the titaniferous slag were in excess of 95%. In line with the proposed process by Jena et al., the vanadium and titanium would thus need to be extracted from the titaniferous slag, while iron is recovered as the corresponding high purity pig iron (Jena, et al., 1994).

Table 6: Chemical compositions of the bulk test slags (wt%)

Test	MgO	Al_2O_3	SiO_2	CaO	$^{\$}TiO_2$	V_2O_5	Cr_2O_3	MnO	$^{\#}FeO$	Total
Target	4.00	13.12	19.69	26.00	37.19	0.00	-	-	0.00	100.00
2	3.43	29.63	12.83	20.73	24.37	0.23	0.06	0.26	7.49	99.05
2*	4.25	13.12	15.89	25.67	30.16	0.28	0.07	0.33	9.28	99.05
3	3.16	7.95	12.40	17.30	22.00	2.90	0.59	0.43	34.20	100.93
4	3.13	7.97	12.30	17.20	22.00	2.90	0.56	0.43	34.30	100.79
5	3.14	7.98	12.50	17.40	22.00	2.93	0.57	0.43	34.40	101.35

Test 2* calculated slag composition after correcting for Al_2O_3 contamination; $^{\$}$Total Ti species ($Ti^{3+}$ and Ti^{4+}) expressed as TiO_2; $^{\#}$Total Fe species (Fe^0 and Fe^{2+}) expressed as FeO

3.3. Mineralogy of the slag products

The backscattered electron microstructures, EDS and XRD results of the titaniferous slags produced in the conventional induction furnace and cold crucible induction furnace are shown in Figure 6. The phase assemblage in the slag produced in the conventional induction furnace included perovskite, rutile, pseudobrookite solid solution, gehlenite, and spinel solid solution [$Mg(Al,Ti,V)_2O_4$]. Although the bulk chemical composition of the produced slag contains a significant content of iron, the observed microstructure does not show iron bearing chemical phases. In addition, the expected pig iron entrainment in the titaniferous slag is also not observed in the microstructure of the slag. The absence of the iron bearing phases on the microstructure can be attributed to the slag inhomogeneity.

According to the phase diagram for titaniferous slags (Goso, et al., 2016b; Jochens, 1967), the produced titaniferous slag with an MgO content of 4.25wt% in the conventional induction furnace should have minimum crystals $Mg(Al,Ti,V)_2O_4$. However, the slag crystallised with $Mg(Al,Ti,V)_2O_4$ as one of the major phases. The excessive crystallisation of the $Mg(Al,Ti,V)_2O_4$ in this titaniferous slag is attributed to the abundant Al_2O_3 in the melt which is attained from the wear of the test crucible. With an MgO content of 4.25wt%, the spinel content in the titaniferous slag would be about 15wt% if it is assumed that all the MgO would be contained in the magnesia alumina spinel structure. It is further assumed that excess Al_2O_3 in the spinel stoichiometry is deported to other phases such as gehlenite and pseudobrookite. With these assumptions, it is anticipated that the upgrading of the produced titaniferous slag using the UGS process would result in the final titania product containing more than 80wt% TiO_2.

The phase assemblage in the titaniferous slag composite produced in the cold crucible induction furnace included perovskite, pseudobrookite, olivine, Fe oxide and iron rich ulvospinel phases.

The content of the spinel phase in the slag can be approximated by the MgO concentration in the slag – this is for estimation purposes only. Assuming that most of the MgO crystallised in the magnesia alumina spinel, the titaniferous slag composite can thus be beneficiated to a titania product with about 90wt% TiO_2.

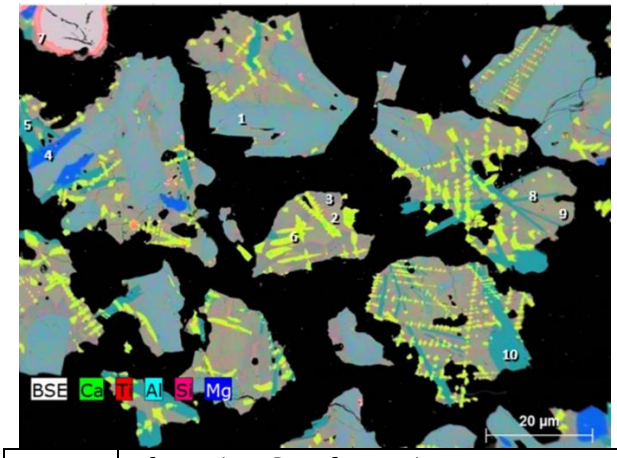

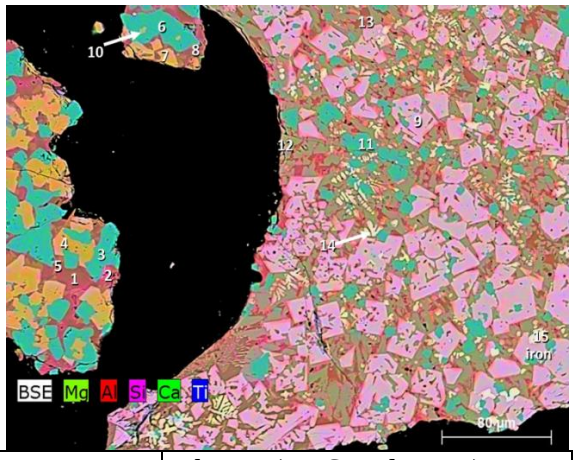

	Phase (EDS and XRD)		Phases (EDS and XRD)
1,3,9	Titanaugite	1,2,5,8,13	Titanaugite
2	Gehlenite	3, 6,10,11	Perovskite
4	Spinel solution [$Mg(Al,Ti,V)_2O_4$]	4,7	Ulvospinel
5,8,10	Pseudobrookite	9	Ferrous pseudobrookite
6	Perovskite	12	Olivine
7	Rutile	14,15	Wustite
	Quartz		
Conventional induction furnace		**Cold crucible induction furnace**	

Figure 6: Backscattered electron microstructure, EDS and XRD results of the titaniferous slags produced in an alumina crucible using the conventional induction furnace and in the cold copper crucible induction furnace

3.4. UGS processing of the titaniferous slag produced in conventional induction furnace

The titaniferous slag produced in the conventional induction furnace in alumina crucible was processed using the best combination of modified UGS conditions determined in previous work (Goso, et al., 2016a), as detailed in section 2.4.

2.3.1 Bulk chemical compositions

The bulk chemical compositions of the untreated and processed intermediate and final products from the UGS processing of the titaniferous slag produced in the conventional induction furnace are given in Table 7. The results show that the produced titaniferous slag could only be upgraded from about 24wt% to 67wt% TiO_2 using the combination of modified UGS conditions established on the EHSV titaniferous slag in the past (Goso, et al., 2016a). From a chemical point of view, this UGS product does not meet the specifications of the feedstock for the chloride process (Pistorius, 2008).

The results in Table 7 also show that the cumulative recoveries of the MgO and Al_2O_3 to residue were adversely significant in excess of 20%. The cumulative recovery of TiO_2 in the beneficiated slag was 76%. It is assumed that in a large scale operation smelting process, there will be no Al_2O_3 contamination. Hence, the UGS process is anticipated to perform better in

terms of beneficiating the titaniferous slags to marketable titania products, preferably for use as feedstock for the production of the chloride pigment.

Table 7: Chemical compositions of the untreated and processed titaniferous slags produced in the current study (wt%)

Sample	Treatment Conditions		Al_2O_3	CaO	Cr_2O_3	FeO	MgO	MnO	SiO_2	TiO_2	V_2O_5
Cast slag	Sized to a range: +150 – 600 µm		29.63	20.73	0.06	7.49	3.43	0.26	12.83	24.37	0.23
Oxidized slag	Oxidation in a fluidized bed, air at 875°C for 2 hours	After	28.65	19.96	0.06	7.96	3.35	0.26	12.66	**24.21**	0.23
	Recovery to residue		98%	97%	101%	107%	99%	101%	100%	100%	101%
Reduced slag	Reduction in a fluidized bed, in CO at 875°C for 0.5 hours	After	28.54	19.96	0.06	7.96	3.35	0.26	12.66	**24.72**	0.23
	Recovery to residue		99%	99%	99%	99%	99%	99%	99%	101%	99%
HCl leach residue	Leach in 20% HCl under reflux at 110°C for 24 hours in s: l of 1:4	After	25.05	4.74	0.00	0.33	4.48	0.09	16.90	**47.45**	0.07
	Recovery to residue		42%	11%	0%	2%	64%	17%	64%	92%	15%
Caustic leach residue	Leach in 2.15 M NaOH at 100°C for 3 hours in s: l of 1:4, calcination at 900°C, 3 hours	After	22.40	5.18	0.00	0.29	3.41	0.08	1.87	**66.90**	0.19
	Recovery to residue		52%	64%	0%	51%	44%	52%	6%	82%	158%
Cumulative recovery to residue			21%	7%	0%	1%	28%	9%	4%	76%	23%

2.3.2 Phase chemistry

The backscattered SEM micrographs, EDS and XRD characterisation results of the oxidative- and reductive roasted titaniferous slag produced in the conventional induction furnace, and HCl and NaOH leach residues are shown in Figure 7 and Figure 8, respectively. After the oxidative roasting, the phase assemblage of the titaniferous slag is like the cast titaniferous slag phase assemblage reported in Figure 6. The observed microstructure of oxidised slag does not show the spinel phase. The spinel phase in the oxidised slag was determined by XRD. The current results support the view that the produced titaniferous slag may have not been completely homogeneous.

After reduction (Figure 7), many phases that were observed in the oxidised slag still existed. However, after reductive roasting, the pseudobrookite phase is decomposed into rutile phases and HCl acid soluble wustite (FeO). Moreover, XRD results suggest that the FeO was further reduced to metallic Fe. Reductive roasting appears to have also decomposed some silicate phases to form quartz. The spinel solid solution is observed in the microstructure of the reduced slag. From the view point of the morphology of phases, the spinel phase of the reduced slag appears to be discrete – other gangue minerals also appear to be totally liberated, and not blocked or encapsulated by the spinel.

The backscattered electron micrograph, EDS, and XRD results of the HCl residue in Figure 8 show that the detrimental elements were incorporated in several phases including olivine, pseudobrookite, spinel and titanaugite phases. Some of the impurity element bearing phases like olivine are typically not inert to chemical treatment. In addition, these phases are still discrete. Thus, the inadequate removal of these impurities can be attributed to the fact that the adopted UGS test conditions may not be optimum as they were not optimized for the current slag (the test conditions were determined using the EHSV slag (Goso, et al., 2016a)), rather than the inertness of the impurity element bearing phases.

The backscattered electron micrograph, EDS, and XRD results of the NaOH residue or the UGS product included in Figure 8 show that the impurities in the upgraded titaniferous slag were incorporated in several phases including quartz, pseudobrookite and spinel. All these phases are still discrete. Hence it may happen that the dissolution of the gangue phases, like quartz, is hampered by that the test conditions were not optimized. .

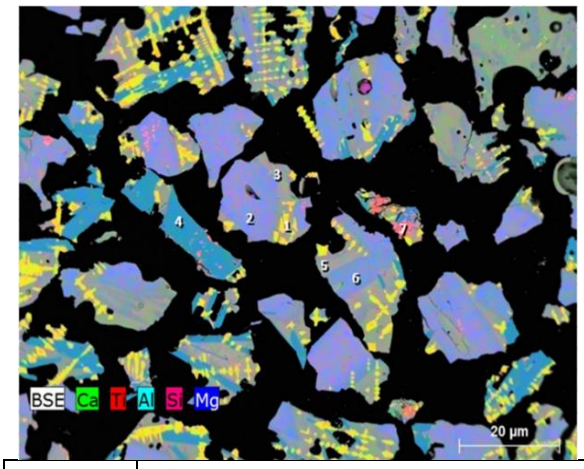

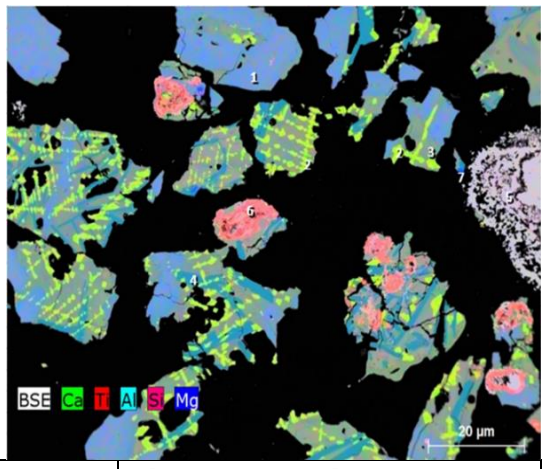

	Phase (EDS and XRD)		Phase (EDS and XRD)
1	Perovskite	1,3,	Titanaugite
2,3,5,6	Titanaugite	2	Perovskite
4	Pseudobrookite	4	Pseudobrookite

7	Rutile	5	Wustite (FeO)
	Spinel	6	Rutile
	Gehlenite	7	Spinel
			Fe
			Quartz
			Gehlenite
Oxidised titaniferous slag		**Reduced titaniferous slag**	

Figure 7: Backscattered electron microstructure, EDS and XRD results of the oxidized and reduced titaniferous slags produced in alumina crucible

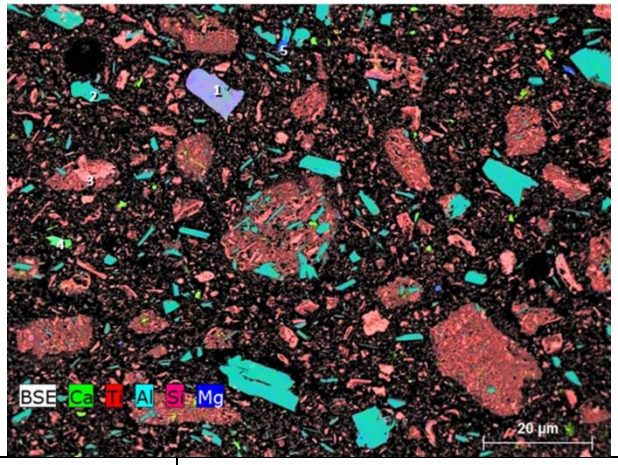

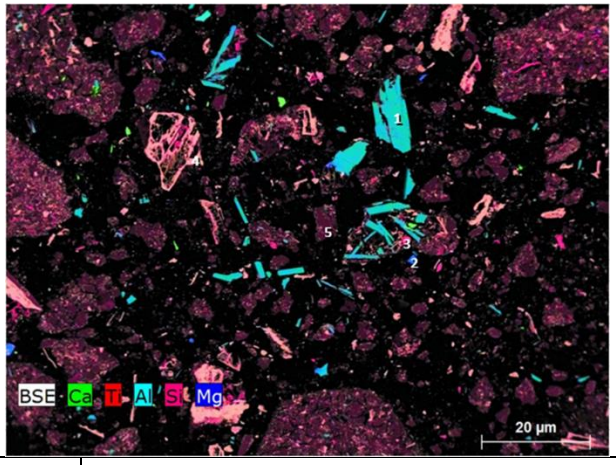

	Phase (EDS and XRD)		Phase (EDS and XRD)
1	Olivine, $(Mg,Ca,Fe)_2SiO_4$	1	Pseudobrookite
2	Pseudobrookite	2	Spinel
3	Rutile	3,5	Quartz
4	Titanaugite	4	Rutile
5	Spinel		
HCl leach residue		**NaOH leach residue – UGS product**	

Figure 8. Backscattered electron microstructure, EDS and XRD results of the HCl and NaOH leach residues of the titaniferous slag produced in alumina crucible

2.3.3 Particle size distribution

The PSDs of the titaniferous slag produced in the conventional induction furnace after processing through the different stages of the UGS process are shown in Figure 9. As was the case with the EHSV titaniferous slag (Goso, et al., 2016a), the curves on the graph show that the PSD of the slag is significantly smaller after the respective leaching stages. The final upgraded titaniferous slag has a D_{95} of 150 µm. In addition to the chemistry point of view, the PSD of the final UGS product is not suitable for use as feedstock for the production of the preferred chloride pigment using the fluidization process.

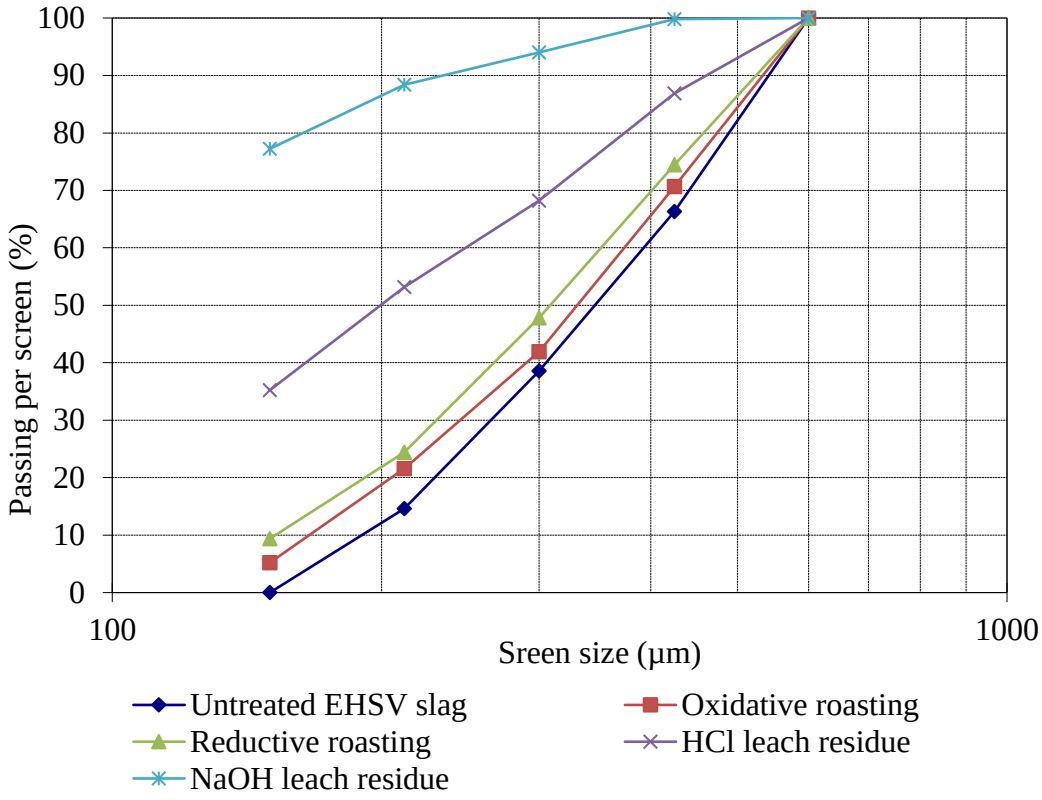

Figure 9. PSD of the UGS process intermediate and final products from the titaniferous slag produced in alumina crucible

3.5. UGS processing of the titaniferous slag produced in cold crucible

The composite of the three titaniferous slag batches produced in the cold crucible induction furnace was used as feed to the UGS process conditions evaluated in this section of the study. The UGS oxidative and reductive roasting conditions were adopted from the previous studies (Goso, et al., 2016a). The effects of the HCl and NaOH leaching times on the upgrading of TiO_2 in this slag were studied and reported in the following subsections.

2.3.4 Oxidative and reductive roasting of titaniferous slag

The backscattered electron images, EDS and XRD analysis results of the oxidised and reduced titaniferous slag produced in the cold crucible induction furnace are shown in Figure 10. In general, there was no significant phase transformation after the two roasting stages. The results however show that after the oxidative roasting, the discrete iron species observed in the cast titaniferous slag, shown in Figure 6, were oxidised to hematite (Fe_2O_3). Hematite was reduced to wustite after the reductive roasting stage. There is no evidence of over reduction in the phase chemistry to suggest that the observed iron reduction may have been accompanied by the adverse reduction of Ti^{4+} to Ti^{3+}. Ti^{3+} is relatively soluble in HCl lixiviant. Thus, if substantial titanium in the slag is in the form of Ti^{3+}, there can be substantial titanium losses to the leachate (Borowiec, et al., 1998; Doan, 1996).

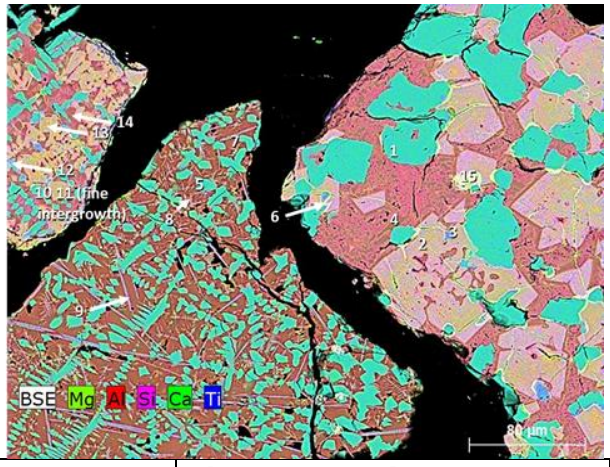

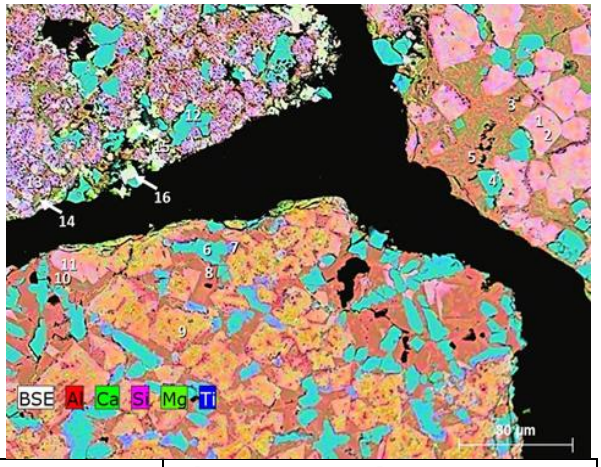

	Phase (EDS and XRD)		Phase (EDS and XRD)
1,5,10,12	Perovskite	1,2,11,13	Pseudobrookite (high Fe)
2,11	Ulvospinel	3,5,8,10	Olivine
3	Rutile	4,6,7,12	Perovskite
4	Olivine	9	Ulvospinel
6,15	Hematite	14	Titanaugite
7,14	Titanaugite	15,16	Wustite
8,9	Ferric-pseudobrookite		
13	Ilmenite		
Oxidized titaniferous slag		**Reduced titaniferous slag**	

Figure 10. Backscattered electron microstructure, EDS and XRD results of the oxidative and reductive roasted titaniferous slag produced in the cold crucible

2.3.5 Effect of HCl leaching time on titania upgrading in the titaniferous slag

The effect of HCl leaching time on the upgrading of TiO_2 in the oxidative-reductive roasted titaniferous slag produced in the cold crucible induction furnace was studied. In these studies, the pulp density and the HCl lixiviant concentration was kept constant at 25 w/v% (or s: l ratio of 1:4) and 20wt%, respectively. The leaching times were investigated at 4, 24 and 48 hours. The results are shown in Figure 11. The results show that the TiO_2 grade in the residue increases with increasing the HCl leaching time. After a reaction time of 48 hours, the TiO_2 grade in the residue had not reached a saturation point. The TiO_2 recoveries to the residue are also very high at more than 90%. The high TiO_2 recoveries in the residue suggest that the concentration of the HCl soluble Ti^{3+} species in the roasted feed slag was favourably low.

The bulk chemical compositions of the HCl leach residues of the slags are given in Table 8. The results show that during the HCl leaching, Mg, Al, Ca, V, Cr, Mn and Fe are effectively removed from the residue. The crucial removal of Mg and Al to very low concentrations or, insignificant concentrations in the case of Mg, suggest that these species were not incorporated into the chemically inert magnesium alumina spinel. As shown in Figure 6 and Figure 10, the spinel structure contained in the cast and roasted titaniferous slag produced using the cold crucible induction furnace is an ulvospinel, i.e. Fe_2TiO_4 – this spinel structure was decomposed by the HCl leaching exercise, resulting in substantial iron dissolution.

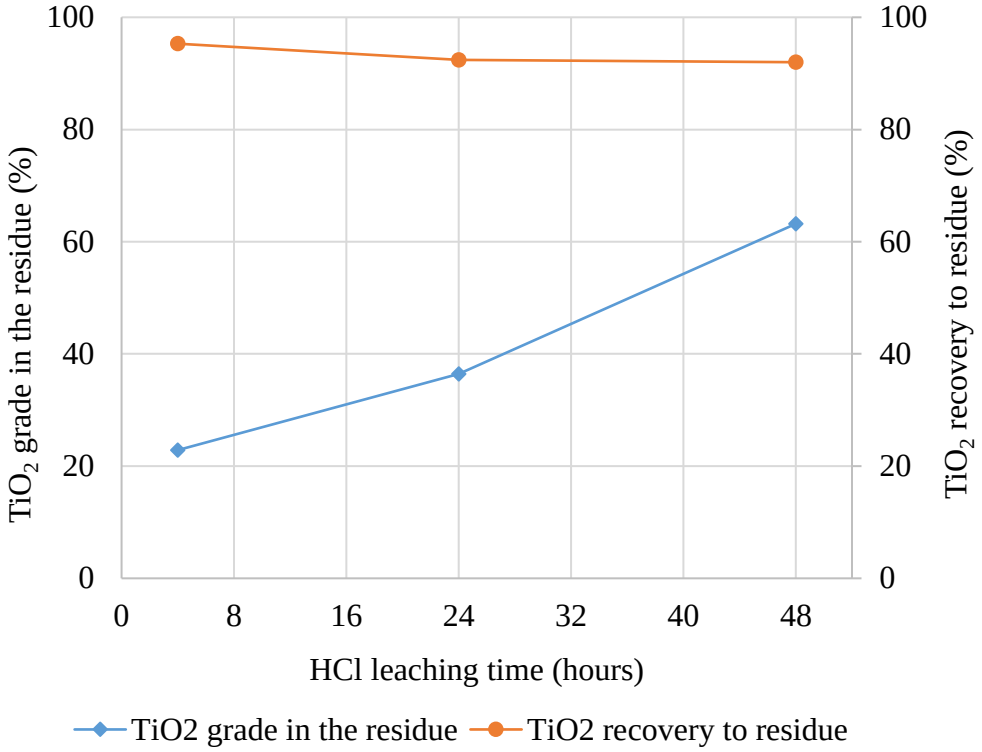

Figure 11. Effect of HCl leaching time on the upgrading of TiO_2 in the titaniferous slag produced in the cold crucible induction furnace

Table 8: Chemical compositions of the slag leach residues produced at different HCl leaching times (wt%)

Leaching time (hours)	MgO	Al_2O_3	SiO_2	CaO	TiO_2	V_2O_5	Cr_2O_3	MnO	FeO
*Feed	2.80	7.22	11.80	15.20	20.20	2.85	0.64	0.43	38.10
4	2.75	7.27	18.11	13.58	22.85	1.46	0.77	0.36	32.85
24	2.37	6.09	17.97	13.74	36.46	2.18	0.73	0.22	20.24
48	0.50	1.45	32.93	0.29	63.18	0.21	0.20	<0.05	1.23

*Oxidative-reductive roast of the composite of titaniferous slags produced in the cold crucible induction furnace

2.3.1 Effect of NaOH leaching time on titania upgrading in the titaniferous slag

The study of the effect of NaOH leaching time on the upgrading of TiO_2 in the oxidative-reductive roasted titaniferous slag produced in the cold crucible furnace was conducted on the HCl leach residue produced after a leaching time of 48 hours. During the kinetic studies, the pulp density and NaOH concentration were kept constant at 25 wt% and 2.15 M, respectively. The NaOH leaching time was investigated at 1, 3, and 24 hours. The results are presented in Figure 12. The results show that the maximum TiO_2 grade of about 91wt% is achieved within an hour of leaching the HCl residue with the NaOH lixiviant. However, the recovery of TiO_2 to the residue decrease with increasing the NaOH leaching time. Hence, NaOH leaching times of more than an hour are not recommended.

Table 9 gives the results of the chemical compositions of the respective UGS products produced after different NaOH leaching times of the HCl leach residue. The results show that

the NaOH leaching exercise effectively and exclusively leached out silicon species from the HCl leach residue. A residual concentration of over 3wt% of SiO_2 remained in the UGS product even at elongated caustic leaching times of 24 hours. The phase of existence of the residual SiO_2 is discussed in the following subsections. The current UGS product containing 90.45wt% TiO_2, which was produced from titaniferous slag fluxed with synthetic lime and had high residual FeO, met the TiO_2 grade specification for the feedstock for the chloride pigment production. However, the SiO_2, Al_2O_3, CaO, and Cr_2O_3 concentrations in the UGS product are higher than the specifications. Further optimisation of the UGS process conditions has a potential to upgrade the TiO_2 and remove the impurities to acceptable levels for the feedstock for the production of chloride pigment.

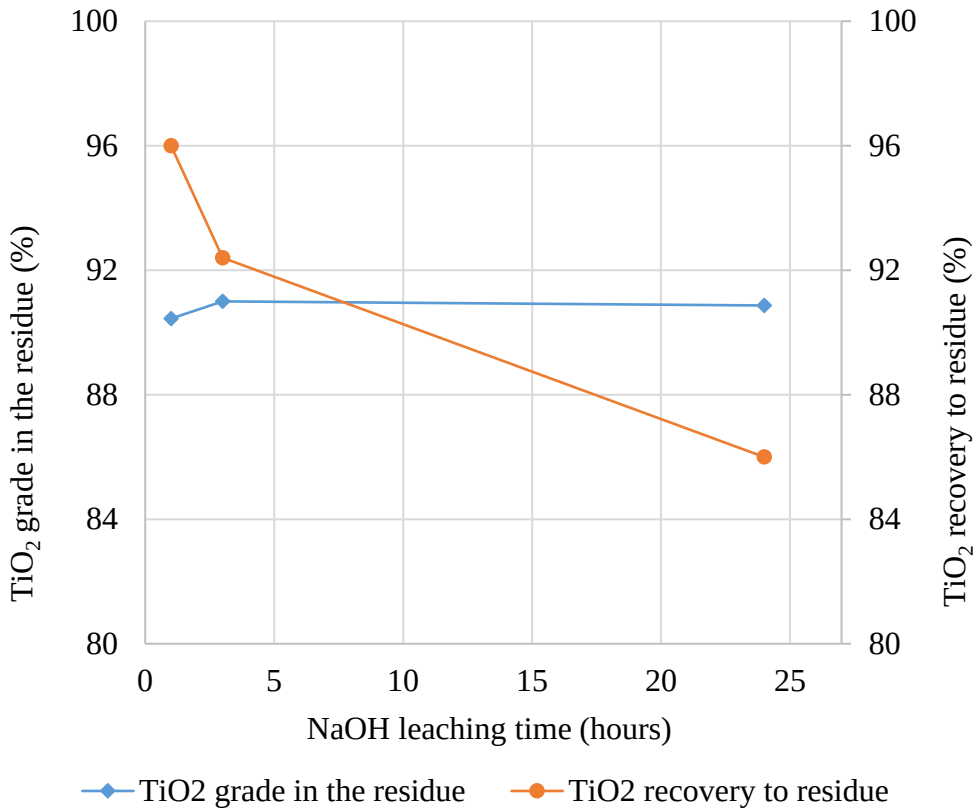

Figure 12. Effect of NaOH leaching time on the upgrading of TiO_2 in the HCl leach residue of the titaniferous slag produced in the cold crucible induction furnace

Table 9: Chemical compositions of the UGS products produced at different NaOH leaching times (wt%)

Leach time (hours)	MgO	Al_2O_3	SiO_2	CaO	TiO_2	V_2O_5	Cr_2O_3	MnO	FeO
*Feed	0.50	1.45	32.93	0.29	63.18	0.21	0.20	<0.05	1.23
1	0.80	1.71	3.77	0.62	90.45	0.32	0.29	0.07	1.98
3	0.86	1.78	3.31	0.72	91.00	0.29	0.28	0.07	1.70
24	0.84	2.04	3.32	0.58	90.87	0.29	0.29	0.07	1.69

*HCl leach residue for the 48 hour test

2.3.2 Bulk chemical compositions

The bulk chemical compositions of the untreated and, processed intermediate and final products from the UGS processing of the titaniferous slag produced in the cold crucible induction furnace are combined in Table 10. The results show that during HCl leaching, Al, Ca, Cr, Fe, Mg, Mn and V are effectively removed from the oxidative and reductive roasted titaniferous slag. During the NaOH leaching, Si-containing species were leached out. However, there were titanium losses of 8% and 4% during the respective HCl and NaOH leaching stages. The titanium losses were attributed to the leaching of Ti^{3+} species. The cumulative recovery of TiO_2 to the UGS product was 83%.

2.3.3 Phase chemistry

The backscattered electron image, EDS and XRD results in Figure 13 show that pseudobrookite, rutile, titanate and quartz were the significant phases in the 48-hour HCl leach residue. The respective phases are primarily composed of Ti and/ or Si species, which were not removed after the HCl leaching. It is important to note that the HCl leach residue did not have the spinel structure. Thus, the ulvospinel observed in the cast and roasted slags is not as inert as the normal magnesium alumina spinel observed in typical titaniferous slags.

The backscattered electron image, EDS and XRD analysis results of the NaOH leach residue or final UGS product in Figure 13 show that this product is primarily composed of rutile, and to a lesser extent perovskite and pseudobrookite. The XRD results showed that the residual Si observed in the chemical analysis results in Table 10 occurred in the titanate ($CaO.TiO_2.SiO_2$) structure, which is a minor phase in the UGS product. The studies conducted for the upgrading of TiO_2 in the titaniferous slag showed that the decomposition, and thus the removal of Si-containing species is not sensitive to an increase in the NaOH leaching time of 1 hour or more. Thus, further testwork is required to investigate the effect of other parameters on the decomposition of the titanate and removal Si values. These test parameters include the NaOH lixiviant concentrate, pulp density, leaching temperature and leaching pressure.

2.3.4 Particle size distribution

The PSD analysis results of the titaniferous slag produced in the cold crucible induction furnace after processing through the different stages of the UGS process are shown in Figure 14. These results show that the PSD of the titaniferous slag is significantly reduced after the HCl and NaOH leaching stages. The final UGS product had a D_{70} of 150 µm.

Though, in terms of the TiO_2 grade, the UGS product meets the specifications for the chloride feedstock, the PSD and other chemical impurities compromise the use of the current UGS product as feedstock for the chloride process.

Table 10: Chemical compositions of the untreated and processed titaniferous slags produced using the cold crucible (wt%)

Sample	Treatment Conditions		Al_2O_3	CaO	Cr_2O_3	FeO	MgO	MnO	SiO_2	TiO_2	V_2O_5
Slag composite	Sized to 600-150 µm		7.97	17.29	0.57	34.30	3.14	0.43	12.39	**22.00**	2.91
Oxidised slag	Oxidation in a fluidized bed, air at 875°C for 2 hours	After	7.51	16.17	0.68	36.14	2.97	0.44	12.05	**21.03**	3.02
	Recovery to residue		97%	97%	122%	109%	98%	107%	100%	99%	107%
Reduced slag	Reduction in a fluidized bed, in CO at 875°C for 0.5 hours	After	7.22	15.20	0.64	38.10	2.80	0.43	11.80	**20.20**	2.85
	Recovery to residue		95%	93%	93%	104%	93%	96%	97%	94.8%	93%
HCl leach residue	Leach in 20% HCl under reflux at 110°C for 48 hours in s:l of 1:4	After	1.45	0.29	0.20	1.23	0.50	<0.05	32.93	**63.18**	0.21
	Recovery to residue		6%	1%	9%	1%	5%	<0.05	82%	92.0%	2%
Caustic leach residue	Leach in 2.15 M NaOH at 100°C for 1 hours in s:l of 1:4	After	1.71	0.62	0.29	1.98	0.80	0.07	3.77	**90.45**	0.32
	Recovery to residue		79%	143%	9%	107%	108%	<0.05	8%	96.0%	100%
Cumulative recovery to residue			4%	1%	1%	1%	5%	<0.05	6%	83%	2%

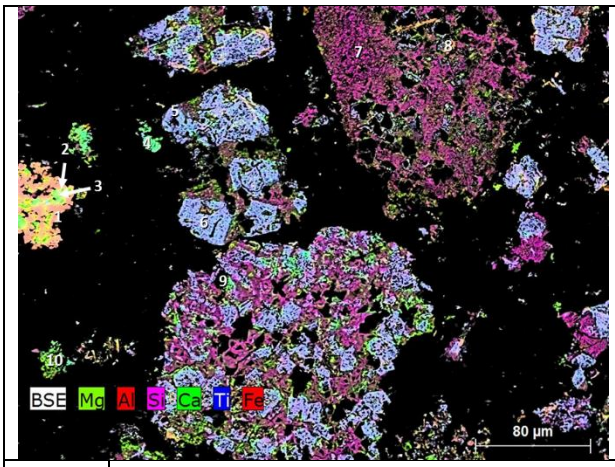

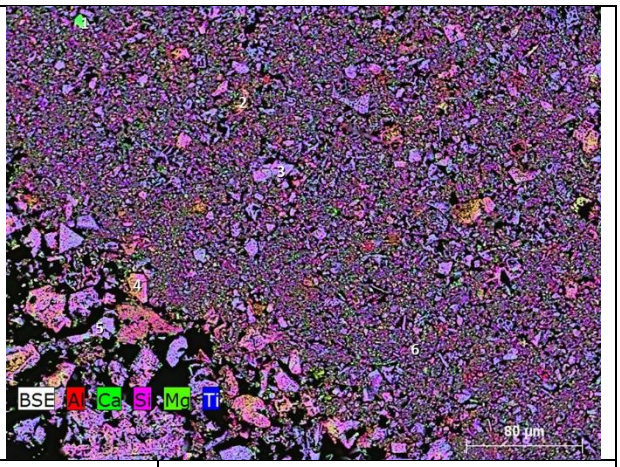

	Phase (EDS and XRD)		Phase (EDS and XRD)
1	Hematite	1	Perovskite
2,8	Ferric-pseudobrookite	2	Pseudobrookite
3,4,9	Titanate	3,4,5,6	Rutile
5,6	Rutile		
7	Quartz		
10	Olivine		
HCl leach residue		**NaOH leach residue – UGS product**	

Figure 13. Backscattered electron microstructure, EDS and XRD results of the 48-hour HCl leach residue and NaOH leach residue (UGS product) from the titaniferous slag produced in the cold crucible induction furnace

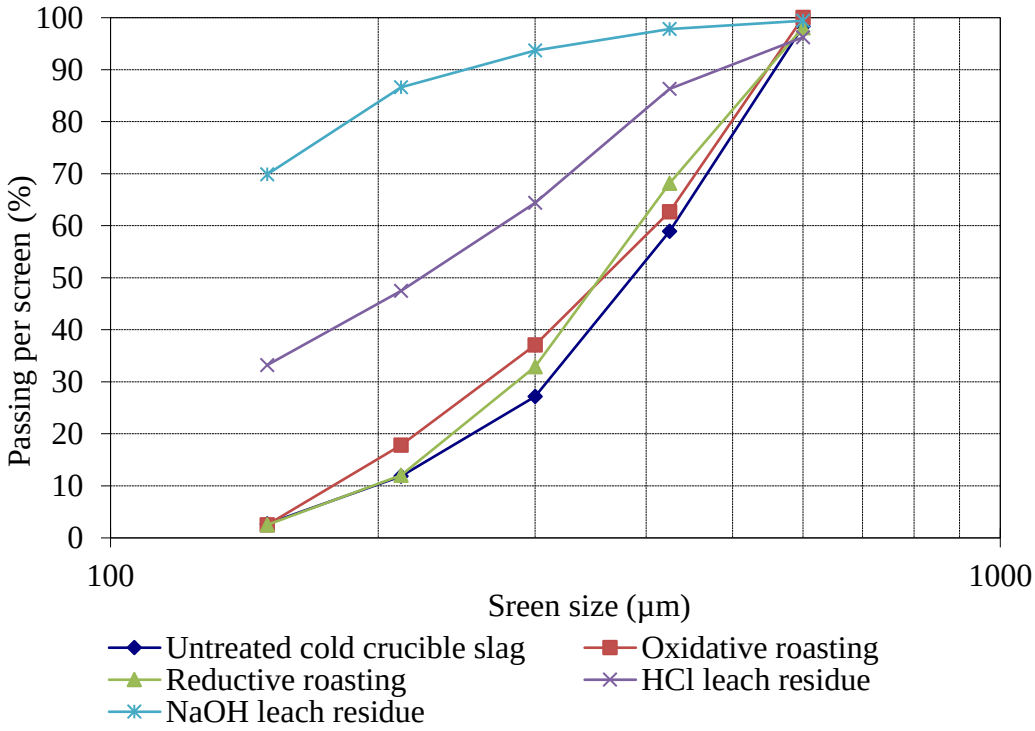

Figure 14. Particle size distribution of the UGS product from titaniferous slag produced in the cold crucible induction furnace

4. CONCLUSIONS AND RECOMMENDATIONS

Investigations into the smelting production of a limestone fluxed titaniferous slag with a suitably low MgO chemistry for subsequent beneficiation using the modified Upgraded Slag (UGS) process to produce a marketable titania material were conducted. The slag produced in alumina crucible was contaminated by the crucible. The high alumina concentrations in the melt promoted the crystallisation of alumina and magnesia as the chemically refractory magnesium alumina spinel. The slag produced in a refractory free copper cold crucible in an induction furnace had high residual iron, mostly from iron metal susceptor and non-equilibrium iron reduction reaction in the titanomagnetite – consequently, the vanadium primarily partitioned to the slag. The high iron concentrations in the slag resulted in the crystallisation of an ulvospinel. Thus, vanadium would need to also be extracted from the titaniferous slag.

Both produced titaniferous slags were acceptable for the purpose of evaluating the feasibility of beneficiating these slags using the UGS process. The best UGS product with 90.45% TiO_2 was produced from the slag samples produced in the cold crucible induction furnace. The TiO_2 grade in this product was sufficiently high; however, the SiO_2, Al_2O_3, CaO, and Cr_2O_3 concentrations were higher, and the particle size distribution was finer than the feedstock specification for the chloride pigment production. Since the UGS product was mainly composed of rutile structure, it was also not suitable for use as feed for the sulfate pigment production, as the rutile is sparingly soluble in sulfuric acid. Further optimisation of the UGS process has a potential to reduce the impurities to levels suitable for feedstock for the preferred chloride pigment production process. Further investigations are also required to study the feasibility of the chlorination of micro-pellets of the UGS product.

5. ACKNOWLEDGEMENT

The paper is published with the permission of Mintek. The authors thank Mintek for financial and test equipment support. Appreciation is also extended to the Norwegian University of Science and Technology (NTNU) in Norway for availing their cold crucible induction furnace for completion of some of the experiments under the INTPART metal production project.

6. REFERENCES

Africa, Mining review, 2017. *Mining review Africa.* [Online] Available at: https://www.miningreview.com/news/nyanza-light-metals-plant-to-provide-titanium-dioxide-pigment-to-africa/ [Accessed 21 May 2017].

Becker, J. H. & Dutton, D. F., 2002. *Recovery of titanium from titanium bearing materials.* United States, South Africa, Patent No. United States Patent 7258847.

Borowiec, K., Grau, A. E., Gueguin, M. & Turgeon, J. -F., 1998. *Method to upgrade titania slag and resulting product.* United States Patent, Patent No. 5,830,420.

Bunting, E. N., 1933. Phase equilibria in the systems TiO_2, TiO_2-SiO_2 and TiO_2-Al_2O_3. *Part of Bereau of Standards Journal of Research,* Volume 11, pp. 719-725.

Doan, P. H., 1996. *Upgraded slag (UGS): implications for TiO_2 feedstock supply.* Industrial Minerals Information Division, Worcester Park, Proceedings of 12th industrial Minerals international congress, pp. 71-76.

Eisenhuttenleute, Verlag Deutscher, 1995. *Slag atlas.* Dusseldorf: Verlag Stahleisen GmbH.

Evans, D. L., 1970. *J. Am. Ceram. Soc.*, 53(7), pp. 418-419.

Fischer, R. P., 1975. Vanadium resources of titaniferous magnetite deposits. *Geological survey professional paper 926-B,* pp. B1-B10.

Fouad, O. A., 2005. Upgrading of a low- grade titanium slag by sulphation roasting technique to produce synthetic rutile. *Acta Metallurgical Slovaca,* 11(1), pp. 14-24.

Gazquez, M. J., Bolivar, J. P., Garcia-Tenorio, R. & Vaca, F., 2014. A review of the production cycle of titanium dioxide pigment. *Materials sciences and applications,* Volume 5, pp. 441-458.

Goso, X. C., Nell, J. & Petersen, J., 2016b. *Review of liquidus temperature and phase equilibria of titaniferous slags at pO_2 applicable to titanomagnetite smelting.* Seattle, TMS, MOLTEN 16.

Goso, X. C., Petersen, J., Nell, J. & Bisaka, K., 2016a. *Scoping study on the upgrading of the fluxed and fluxless titaniferous magnetite slags using the 'upgraded slag' process.* Cape Town, Hydrometallurgy.

Habashi, F., 2002. *Textbook of Pyrometallurgy.* Quebec: Metallurgie Extractive Quebec.

Hassell, D. J. et al., 2016. *Extraction of products from titanium-bearing minerals.* For every kind of national protection available, Patent No. WO 2016/007021 A1.

Jena, B. C., Dresler, W. & Reilly, I. G., 1994. Extraction of titanium, vanadium and iron from titanomagnetite deposits at Pipestone lake, Manitoba, Canada. *Minerals Engineering,* 8(1), pp. 159-168.

Jochens, P. R., 1967. *Contribution to the knowledge of the equilibrium and non-equilibriuim behaviour of titaniferous slags,* Johannesburg, South Africa: University of Witwatersrand, Department of Metallurgy. PhD thesis.

Kelly, B. F., 1993. Ironmaking at BHP New Zealand Steel Limited, Glenbrook, New Zealand. *In Australasian Mining and Metallurgy,* 1 (The Sir Maurice Mawby Memorial), pp. 348-353.

Kirillova, S. A., Almjashev, V. I. & Gusarov, V. V., 2011. Phase relationships in the SiO_2-TiO_2 system. *Russian Journal of Inorganic Chemistry,* 56(9), pp. 1464-1471.

Maphutha, M. P., Ramaili, M., Sitefane, M. B. & Goso, X. C., 2017. The effect of magnesia and alumina crucible wear on the smelting characteristics of titaniferous magnetite. *The journal of the Southern African Institute of Mining and Metallurgy,* 117(7), pp. 649-655.

Massazza, F. & Sirchia, E., 1958. *Chim. Ind.,* Volume 40, pp. 367-380.

Moskalyk, R. R. & Alfantazi, A. M., 2003. Process of vanadium:a review. *Minerals Engineering,* Volume 16, pp. 793-805.

NTMK, 2003. *Specialization: Nizhniy Tagil Iron and Steelworks.* [Online] Available at: htt://www.ntmk.ru/en/manufacture/specialization.php [Accessed 24 03 2015].

Pistorius, P. C., 2004. *Equilibrium interaction between freeze lining and slag from ilmenite smelting.* Cape Town, The South African Institute of Mining and Metallurgy, pp. 237-242.

Pistorius, P. C., 2008. Ilmenite smelting: the basics. *The Journal of The Southern African Institute of Mining and Metallurgy,* Volume 108, pp. 35-43.

Pistorius, P. C., 2011. Titania slag smelting and calcination of crude zinc oxide: examples of processing under thermodynamic and kinetic constraints". *Proceedings of the second international slag valorization symposium, Leuven Belgium,* pp. 263-270.

Roskill, 2003. *The economics of titanium minerals and pigments.* s.l.:Roskill information Ltd.

Roskill, 2010. *Vanadium: Global industry market and outlook, 12th Edition.* s.l.:Roskill information services Ltd.

Steinberg, W. S., 2008. *University of Pretoria.* [Online] Available at: http://repository.up.ac.za/bitstream/handle/2263/26090/dissertation.pdf;sequence=1 [Accessed 10 10 2016].

Steinberg, W. S., Geyser, W. & Nell, J., 2011. The history and development of the pyrometallurgical processes at Evraz Highveld Steel and Vanadium. *Journal of the Southern African Institute of Mining and Metallurgy,* Volume 111, pp. 63-79.

Sui, Z. et al., 2004. *Feasibility of recovering metals from associated slags.* Cape Town, South Africa, VII International conference on molten slags fluxes and salts, The South African Institute of Mining and Metallurgy.

Taylor, P. R., Shuey, S. A., Vidal, E. E. & Gomez, J. C., 2006. Extractive metallurgy of vanadiun-containing titaniferous magnetite ores:a review. *Minerals and metallurgical processing,* 23(2), pp. 80-86.

Van Dyk, J. P., 1999. *Process development for the production of beneficiated titania slag,* Pretoria, South Africa: Dissertation submitted for the degree Philosophiae Doctor in metallurgical engineering at the department of materials science and metallurgical engineering of the University of Pretoria.

Van Vuuren, D. S. & Tshilombo, G. T., 2011. Nitriding of ilmenite and high-grade slag fines. *Journal of the South African Institute of MIning and Metallurgy, South Africa,* Volume 111, pp. 173-181.

Wang, M. et al., 2006. Selective enrichment of TiO_2 and precipitation behavior of perovskite phase in the titania bearing slag. *Trans.Nonferrous Met.Soc.China,* Volume 16, pp. 421-425.

Wang, Y., Qi, T., Chu, J. & Zhao, W., 2010. Production of TiO_2 from $CaTiO_3$ by alkaline roasting method. *Rare metals,* 29(2), pp. 162-167.

Xiao-hua, L. et al., 2008. Kinetics of the leaching of TiO_2 from Ti-bearing blast furnace slag. *J China Univ Mining & Technol,* 18(2), pp. 275-278.

Zhang, L. et al., 2007. Recovery of titanium compounds from molten Ti-bearing blast furnace slag under the dynamic oxidation condition. *Minerals Engineering,* Volume 20, p. 684–693.

Zhang, L. et al., 2006. Effect of perovskite phase precipitation on viscosity of Ti-bearing blast furnance slag under the dynamic oxidation condition. *Journal of crystalline solids,* Volume 352, pp. 123-129.